Sensors & Actuators: A. Physical 345 (2022) 113779

Contents lists available at ScienceDirect

Sensors and Actuators: A. Physical

journal homepage: www.journals.elsevier.com/sensors-and-actuators-a-physical

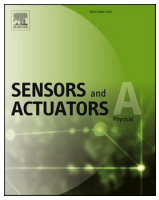

Adaptive reversible composite-based shape memory alloy soft actuators

Mohammadreza Lalegani Dezaki [a], Mahdi Bodaghi [a,*], Ahmad Serjouei [a], Shukri Afazov [a], Ali Zolfagharian [b]

[a] Department of Engineering, School of Science and Technology, Nottingham Trent University, Nottingham NG11 8NS, UK
[b] School of Engineering, Deakin University, Geelong 3216, Australia

ARTICLE INFO

Keywords:
Shape memory alloy
Composite structure
Smart actuator
Soft gripper
3D printing
Fused deposition modelling

ABSTRACT

This research demonstrates how a combination of two-way shape memory alloy (SMA), low-temperature liquid epoxy cure composites, and fibre reinforced plastic (FRP) may be utilised to create a novel reversible actuator with built driven functionality. The novelty of this work is that the actuator can reverse its original shape and be mounted on different customized structures. The strategy is based on a knowledge of SMA wires and the manufacturing principle underlying composite structure, as well as experiments to see how soft SMA-FRP can be programmed to bend. The folding mechanism is studied in terms of fabrication factors such as SMA training and strong interfacial bonding between SMA and epoxy resin, which influence the programming process and shape change. The two-way SMA wires are trained using the pre-straining method to programme the SMAs. The technique has been used to assemble the SMA wires with bond reliability to enhance the actuator interface's thermal behaviour. The SMA elements are directly inserted into FRP strips and epoxy resin is used as an adhesive, resulting in dynamic hybrid composites. The module is actuated using an electrical board with a current value between 3 and 6 A. The robustness, controllability, mechanical properties, and 500 life cycles of the actuator are tested. Results indicate a bending angle of 58° with 30 mm of deflection in 7 s after actuating the module. Also, 3D printing is used to print a gripper inspired by human fingers and a structure to lift various weights. The actuator's performance as a soft gripper is reliable in terms of grasping objects of different shapes.

1. Introduction

Soft robots have been inspired by the outstanding functions of animals, ranging from muscle contraction/relaxation to mobility [1–3]. They are capable of a wide range of tasks, including sophisticated control in enclosed spaces and unfamiliar situations [4]. Soft robots differ dramatically from conventional or rigid manipulators in terms of mechanisms, fabrication, and control strategies. Soft actuators and smart materials with a wide range of capabilities and manufacturing processes have been created [5]. Shape memory materials [6], shape memory alloys (SMAs) [7], liquid metals [8], hydrogels [9], and 2D materials [10], which can be activated by a variety of external stimuli, are promising options to be used as a soft gripper. The power of soft robotic grippers is derived using magnetic and/or electric fields, pneumatic and/or hydraulic actuators, and thermal actuators [11–13].

SMAs are classified as smart materials as they can undergo direct electrothermal actuation with high durability. Also, SMA actuators have a number of benefits, including low driving voltages, biocompatibility, compact size, and noise-free operations, making them ideal for a wide range of applications [14,15]. SMAs are a class of heat-activated smart materials that rely on the shape memory effect. This means that to make the actuator move quickly, a high current is employed to produce different robots or complex deployable structures [16–18]. However, in real-world applications, their performance is unsatisfactory [19,20]. The nickel-titanium (NiTi) alloy has been widely employed in the design of SMA actuators because of its improved strain properties (up to 7 %) [21].

A solid-state shape transition causes the shape memory effect (SME) in a SMA. A SMA is austenitic (hard) and martensitic (relatively soft) above and below a particular transition temperature, respectively [22–24]. A twinned structure is formed by the material grains. The alloy may be readily deformed to a new shape in the martensitic phase, and the crystalline microstructure de-twins as grains reorient [25,26]. As long as the temperature remains consistent, the new form will persist. The alloy converts back to the austenite phase if it is heated above the transition point, regaining its previous shape [27,28]. SMAs differ in

* Correspondence author.
E-mail address: mahdi.bodaghi@ntu.ac.uk (M. Bodaghi).

https://doi.org/10.1016/j.sna.2022.113779
Received 3 June 2022; Received in revised form 15 July 2022; Accepted 23 July 2022
Available online 23 July 2022

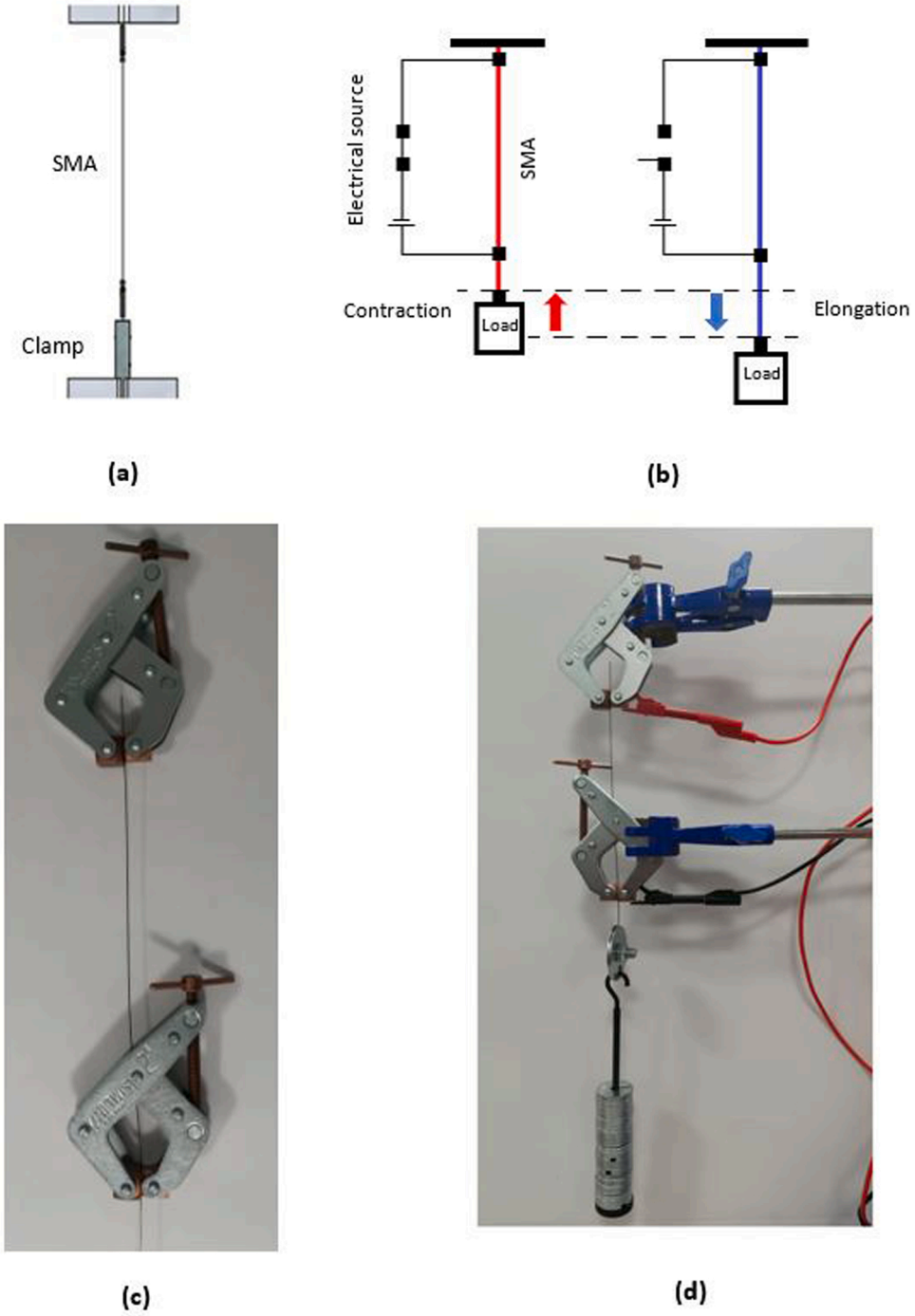

Fig. 1. Schematic of (a) simple tensile test of SMA wire and (b) training of SMA wire. (c) Clamping SMA wire and (d) experimental procedure of SMA training using weight.

their shape-memory effect. One-way and two-way shape memory are two frequent phenomena. While costly training is required for the two-way effect, basic pre-straining is sufficient for the one-way effect. When a one-way SMA is cold, it may be bent or stretched and retain its shape until it is heated over the transition temperature. When heated, the form returns to its original state [29].

Despite the limited linear stroke of SMAs, a large deformation can be achieved by integrating them into a polymeric matrix [30,31]. In a single actuator, numerous SMA wires can be employed to create twisting or bending [32,33]. Also, SMAs are attractive alternatives for light-weight devices and particular applications where design space is limited because of their comparably low specific weight. As an example, Lee et al. [34] developed a wire-based SMA soft actuator with a length of up to 350 mm, which was able to bend up to 400° with 0.89 N tip force. Modabberifar et al. [35] utilised a SMA-wire-based actuator to put a shear strain on the gecko-like adhesive pads in a gripper for grabbing flat items. Liu et al. [36] proposed a novel SMA-based three-finger gripper with variable stiffness. Results indicated that the gripper grasped items of various shapes and weights, and the gripper's maximum force was raised by nearly ten times by employing the variable stiffness joints. Niu et al. [37] developed SMA/PDMS soft actuators with dual-stimulus responsiveness. This study showed that instead of using linked SMA wire configurations, the gripper allowed for reversible actuation using only single SMA wires.

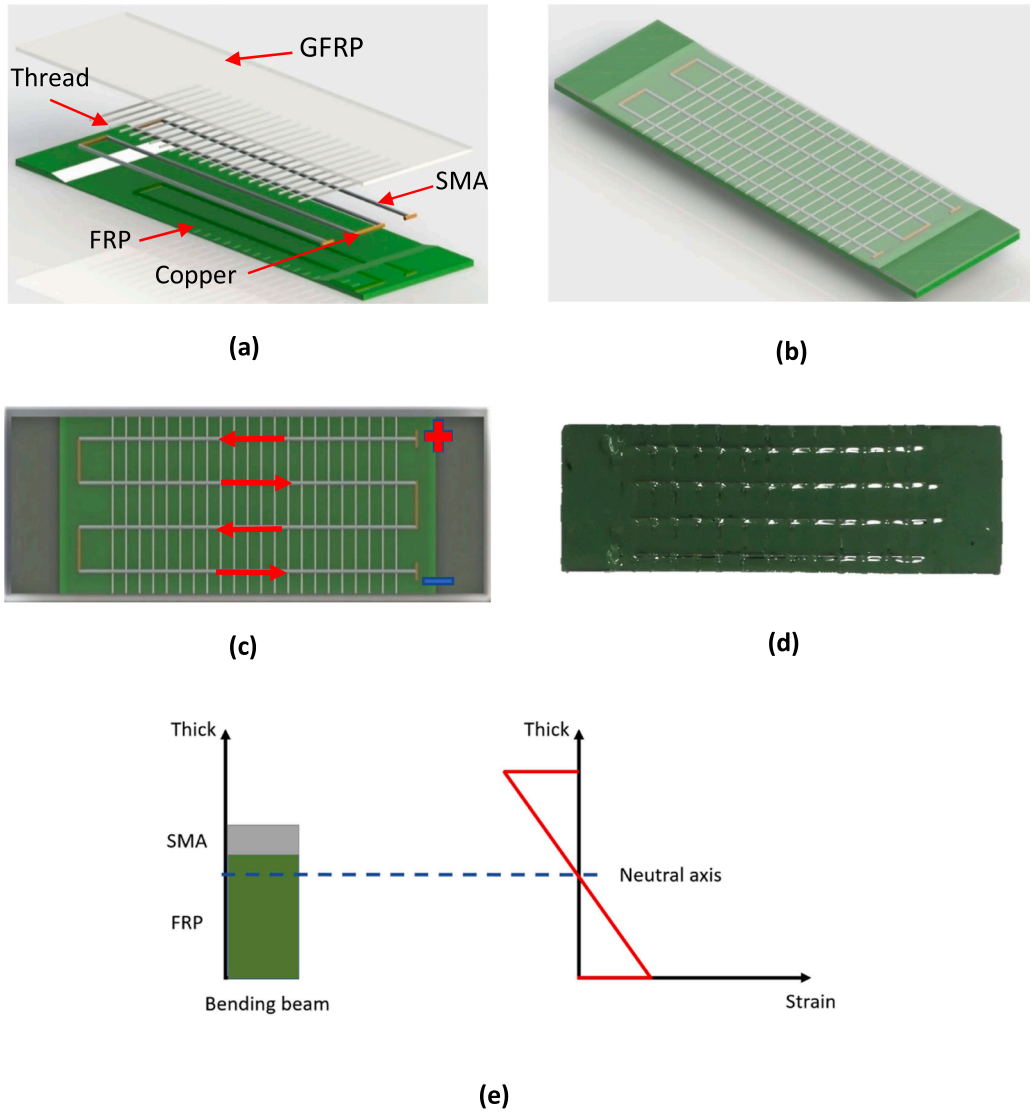

Fig. 2. (a) 3D schematic of the SMA actuator's components. (b) Integration of the SMA actuator with adhesive epoxy. (c) Electrical current direction in the SMA grid. (d) Final SMA-FRP actuator. (e) Cantilever behaviour of SMA and FRP.

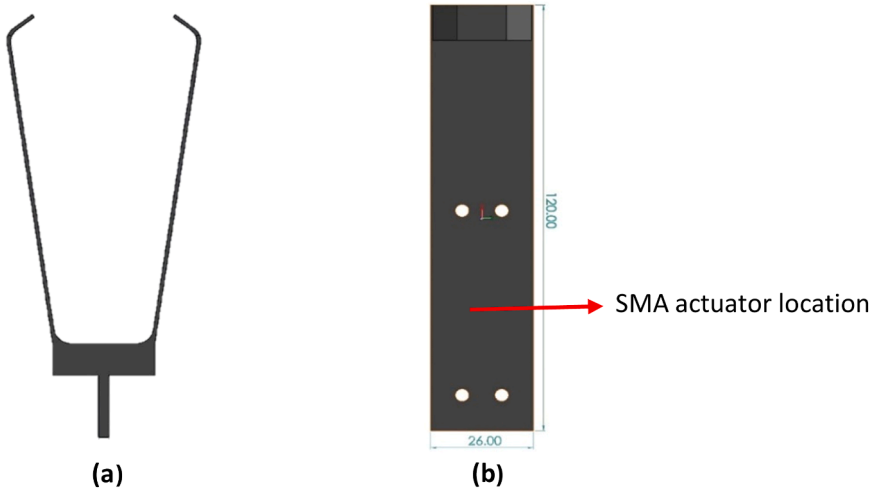

Fig. 3. Design of the 3D printed (a) gripper and (b) base structure.

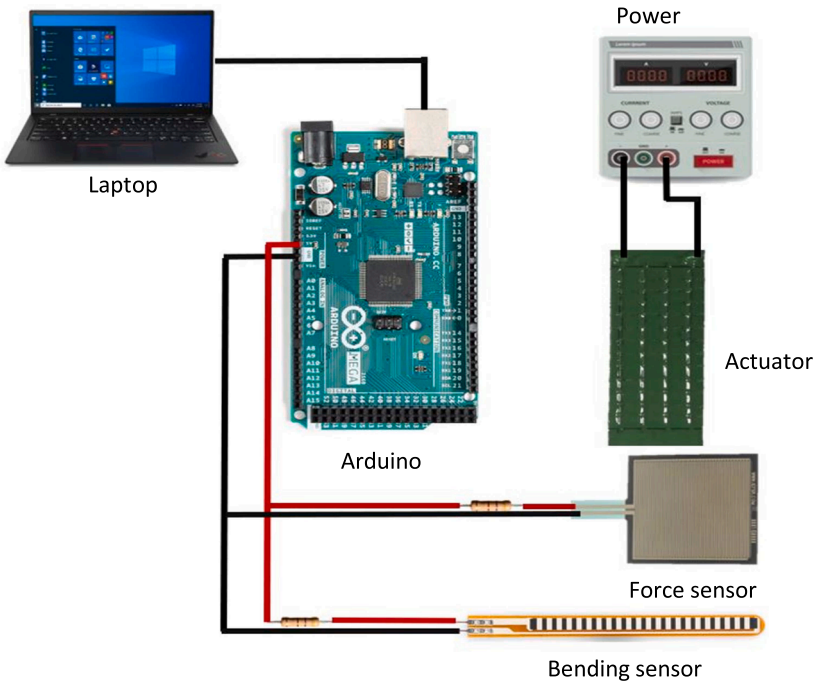

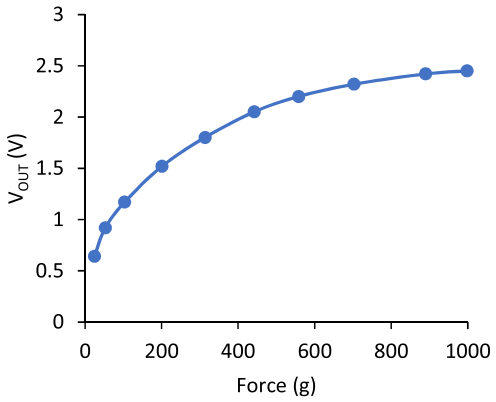

Fig. 4. (a) Schematic of electrical board to control the actuator. (b) Output voltage and force curve of FSR sensor using different weights.

Fibre-reinforced plastics (FRP) have been widely used in different applications due to their high performance and properties [38,39]. In the realm of actuator materials for active composites, SMAs provide prospective performance in terms of achievable strain and stress. As a result, it is possible to combine them with other materials. SMA wires are frequently inserted into various matrix materials, such as epoxy resin and laminated FRP composite materials, to create an intelligent composite or smart structure. The specific energy density is the most important technical parameter in the application of shape memory materials in FRP. SMA has a greater specific energy density (10 MJ/m^3) than shape memory polymer (SMP) (0.1 MJ/m^3) [40]. Hence, SMA is a promising material for quick actuation of FRP with reasonable shape deformability. Furthermore, they have exceptional chemical stability, low brittleness, and thermomechanical characteristics, making them ideal for use in adaptable FRP constructions [41].

Rogers et al. [42,43] pioneered the use of SMA wires in FRP construction in the early 1990 s. Many studies have looked at incorporating SMAs into composites since then [44–46]. Ashir et al. [47] developed an adaptive hinged FRP (AHFRP) integrated with SMA hybrid yarn. Results showed that by extending the hinged width of AHFRP by two and three times from the hinged width of 40 mm, the maximum deformation was raised to 42.7 % and 64.6 %, respectively. Mersch et al. [48] created SMA-based elastomeric actuators which were able to achieve a bending angle of 270° at a power input of 18 W. Araújo et al. [49] manufactured carbon-fibre-reinforced polymers (CFRP) integrated with NiTi SMA wire actuators in a single direction. The samples exhibited standard thermal buckling behaviour, which caused the beam specimen's tip deflection to increase as the temperature rose to 100 °C. A bigger and more stable decrease in thermal buckling was found in CFRP integrated with SMA wires. A specified deformation in a FRP may be introduced with little effort by using a SMA wire as an actuator. However, there are some difficulties to clamp the SMA wire due to the slippage. Bettini et al. [28] demonstrated how to resolve difficulties with SMA wire embedding in carbon fiber/epoxy laminates. Two stable conformations can be found in an unsymmetrically thin FRP sheet. One of these conformations has high stiffness against compression for a certain load direction, whereas the

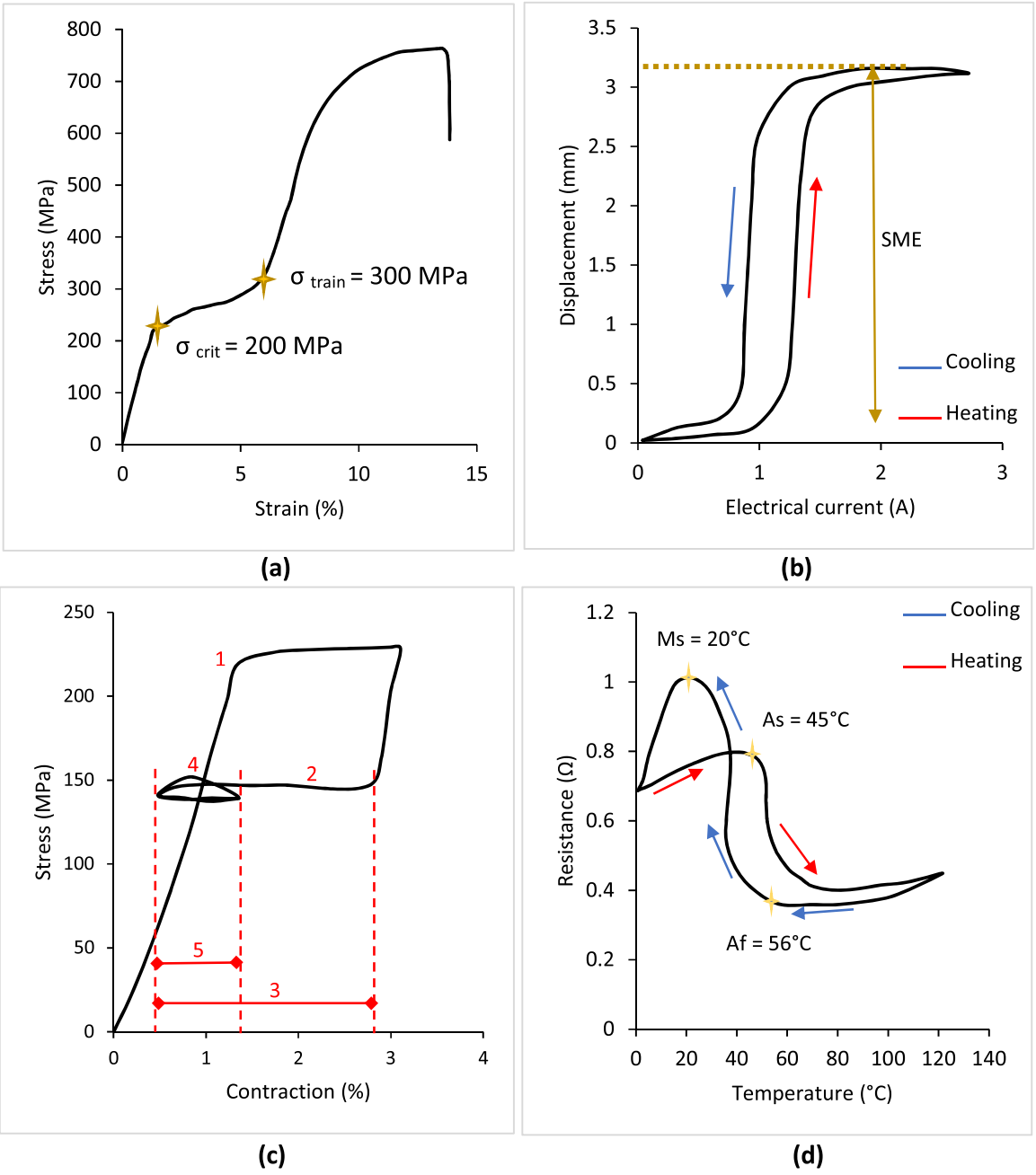

Fig. 5. (a) Stress-Strain of the SMA wire. (b) Contraction and expansion of the SMA wire. (c) Stress-strain curve of heat-activated contraction of the SMA wire. (d) Phase transformation of the trained SMA wire.

other is already bent, resulting in low stiffness against deformation. It helps SMA wires bend the composite structure easily by joule heating and enables high forces and a deflection of several percent. To achieve optimal performance in integrated SMA–FRP composite structures, several aspects must be considered. It is necessary to examine the actuator components' activation and manufacturing processes.

In this study, we show how integrated SMA wires with FRP can be used as actuators to drive a polymeric matrix. The feature of this smart module is the reversibility and high energy density of two-way SMA wires [50]. This gives designers more flexibility when it comes to developing actuators that meet the requisite bending angle and force parameters. The pre-straining test is used to characterise and programme the SMA wires mechanically. Electrical activation of the actuator in a rectangular shape and the performance of the SMA wires in the FRP module are investigated to verify bending deformation and force effects. The advantage of this actuator is that it can be mounted on a customised structure with different shapes. Also, this SMA module is mounted on a 3D-printed structure and used to grab a variety of items. The key contributions of the essay are listed below:

- Studying the characteristics and mechanical properties of the two-way SMA wires.
- SMA wire training is conducted using a pre-straining method to programme the NiTi alloys.
- Development of a novel composite structure using SMA wires and composite plastics and resin which can be mounted on different structures.
- Design and manufacturing of fast responsive composite-based actuator.

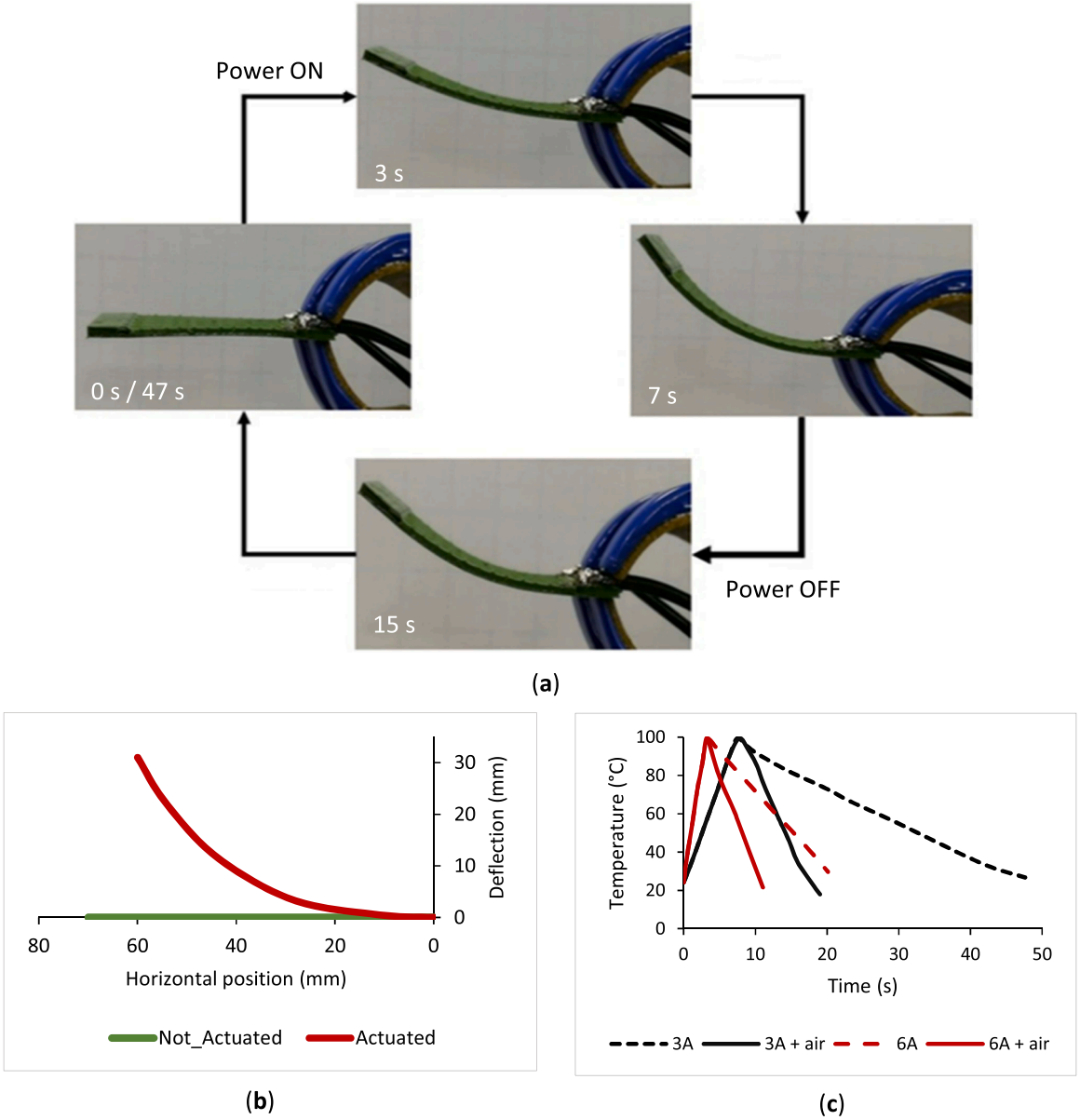

Fig. 6. (a) Deflections of the SMA-FRP actuator in different stages with a current of 3 A. (b) Measured deflection of the actuator with 3 A. (c) Thermal buckling of the actuator with and without air.

- To operate the actuator and provide data, a control system, bending, and force sensor are developed.
- Design and 3D printing of structure and a gripper inspired by human fingers to evaluate the performance of the actuator.
- The performance of soft actuators in terms of bending, tip force, and the life cycle is measured using experimental data for both design and manufacturing processes.
- The ability of the actuator as a gripper is investigated accordingly.

2. Materials and method

2.1. SMA training

The pre-straining, as well as any other treatment of the actuators throughout processing, must be done with the overarching goal of assuring actuating functionality. A SMA round wire with a 0.5 mm diameter from SmartFlex® is used in this work. The SMA wires feature some portion of the two-way effect. However, the use of a bias force is required to fully and timely recover the cold length. To eliminate any earlier active deformation, the SMA wires are heated up to 120 °C (well above the activation temperature) with a current of 6 A, and then cooled to room temperature [49]. Then, a Shimadzu AG-X plus machine is used and TRViewX records displacement accordingly. First, to estimate the stress level for the thermal cycling under the continuous load training technique, a simple tensile test is performed with a 100 mm SMA wire at room temperature with a strain rate of 1 mm/min. The pre-straining training is accomplished to programme the SMA wire before patching on FRP [49,51].

A 50 mm free length of SMA wire is chosen while one side of it is attached to the clamp and the other side is loaded. A TENMA DC power supply is used to heat up the wire for different cycles with a current of 3 A using patches of metal in the isolating clamps. Fig. 1(a) and 1(b) show the schematic of the experimental procedure. During the straining of thin SMA wires, the forming strain, and their expansion can be monitored. Two KANT TWIST clamps are used to clamp the SMA wires as shown in Fig. 1(c). The second clamp is just for adjusting the wire and the needed length throughout the procedure. The holders' materials are plastic and wood. Fig. 1(d) shows the components of SMA training

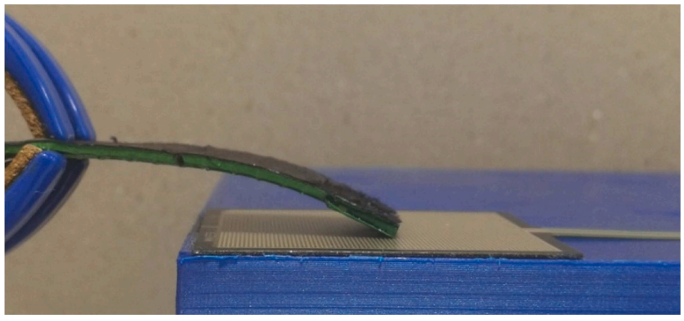

(a)

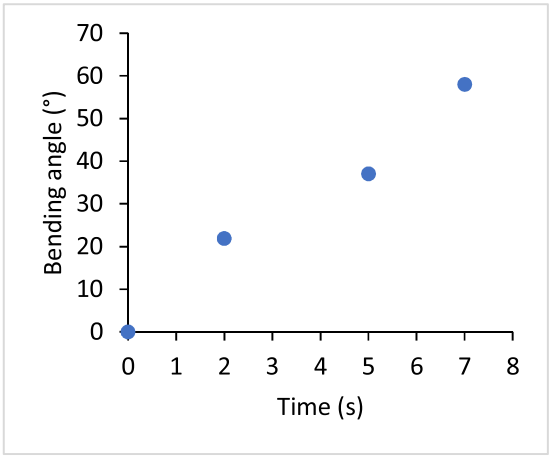

(b)

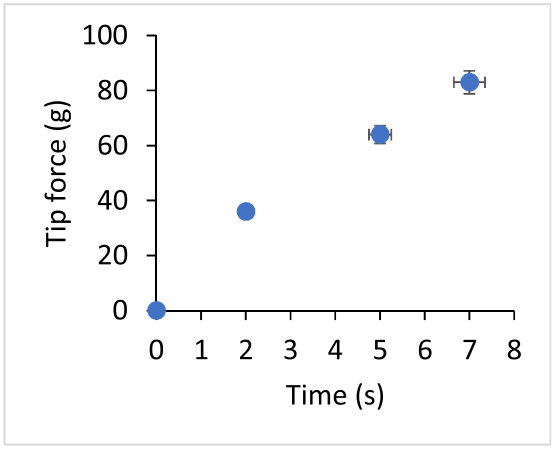

(c)

Fig. 7. (a) Force measurement using FSR sensor. (b) Bending angle of the actuator using 3 A current in different stages. (c) Actuator's tip force in different stages with 5 % error.

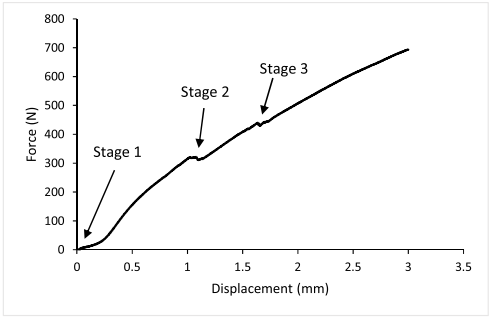

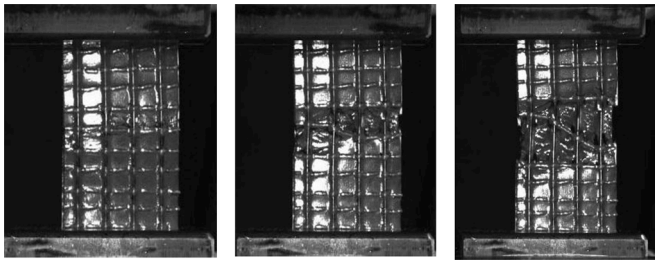

(a)

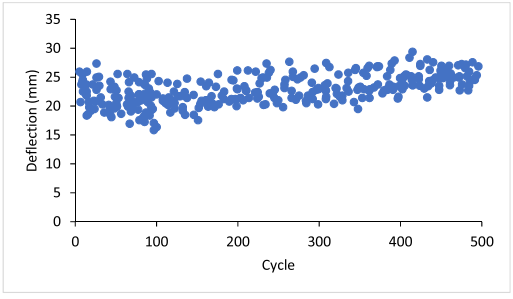

(b)

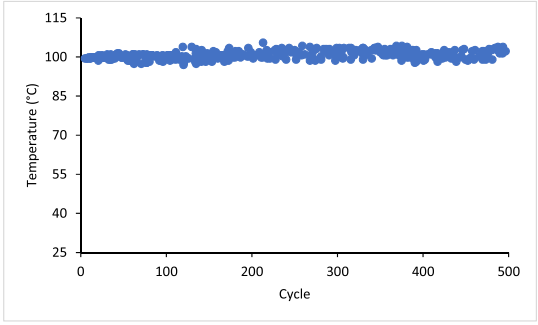

(c)

Fig. 8. (a) Tensile test of the actuator in different stages. (b) Tip deflection and (c) temperature recordings during fatigue tests.

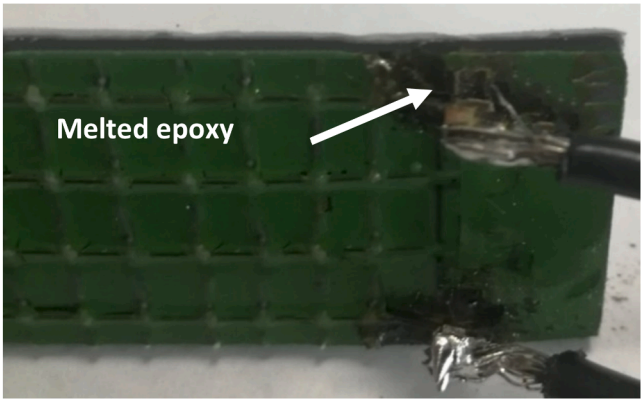

Fig. 9. Overheating damage to the actuator.

accordingly. The same clamps are used for the tensile test and two-piece rubbers are used to isolate the clamps to achieve accurate results.

In each test, the wire is repeatedly heated to a hot condition and then cooled with outside air. With regard to the hot state, it is made sure that the temperature is over 70 °C, which is significantly above the transition temperature, and that the actuation movement has come to a complete halt. For the cold state, a temperature of 25 °C is set. With regard to the cold state, a temperature of 26 °C was established. SMA elongation is measured by TRViewX to guarantee that the whole strain of the SMA wire is recorded. The electrical resistance is determined by recording the activation current and voltage drop along the wire, and the temperature is monitored using a thermometer. The goal of these procedures is to determine the SMA material's maximum possible actuation performance for a single actuation. The wire is heated to a hot state many times throughout each test, and then cooled with air. The temperature should be well above the transition temperature, and the actuation motion is stopped at some point. The integration of SMA with FRP is discussed in the next section.

2.2. Integration of SMA with FRP

For all the trials, a similar test setup is employed. Apart from the high actuation stresses that can be achieved, there are significant benefits in terms of FRP integration when SMA material is utilised in wire form [39, 52,53]. A flat FRP sheet is bent by SMA wire actuators to illustrate the performance of SMA-FRP composites. FRP allows for the creation of a bistable structure using an asymmetric layup in different applications. As a result, a thin sheet made asymmetrically has two stable conformations. One of these conformations has high stiffness against compression for a certain load direction, whereas the other is already bent, resulting in low stiffness against deformation. The actuator module is worked with a simple electrical connection while it has minimal size and weight. The ideal active SMA-FRP structure is achieved which has a repeatable actuation cycle with high deformation.

Fig. 2(a) shows the schematic of the manufacturing procedure. The wire clamping procedure is the same as reported in Araújo et al. [49]. Copper wires are soldered to the SMA wires to ensure an equal distribution of electricity throughout the sample. This allows for better stiffness, strength, and electrical contact at the same time. Equal size of threads is used with a distance of 1 mm to have a better stable actuator. A glass fibre-reinforced plastic (GFRP) is used as a cover for the whole actuator. The use of a GFRP guarantees that appropriate electrical insulation is maintained. Then, the SMA grid is pressed with an adhesive curing epoxy resin (Araldite) with green dye colour and hardener at room temperature for 48 h. The operating temperature of epoxy resin, FRP, and GFRP is up to 150 °C which prevents melting while the SMA wires are heated. Extra layers of FRP are employed on two sides of the actuator to increase the adhesive bonding and stability in loading (See Fig. 2(b)). The size of the actuator is 70 mm in length, 20 mm in width, and its weight is 3 g.

Any hot-curing procedure that exceeds the austenite finish (A_f) temperature causes the structural phase transition in the SMA material. Precautions must be taken during the manufacturing process to avoid the shape changing and the resultant actuating action. In this system, the entire structure is powered by only two electrical connectors (see Fig. 2 (c)). If the stiffness of the structure, the temperature, and the applied strain of the SMA actuator are all the same at every place, a homogenous deformation is obtained using an integrated structure. The thickness of the whole product should not be more than 2 mm which provides difficulties in bending or failure without buckling. Hot curing activates SMA wires; hence, the adhesive epoxy contact between FRP and SMA filaments must be cured at a low temperature. The final actuator is shown in Fig. 2(d). Finally, the actuator is tested under a tensile test with a strain rate of 1 mm/min to investigate its mechanical properties.

The contact between the implanted SMA actuator wire and the surrounding adhesive matrix induces a stress distribution. Because of the abrupt increase in stiffness, the stress concentrations near the margins are highly noticeable. One way to ensure this loading in the joint is to distribute stresses across a suitably broad surface area, for as by reducing the diameter of the SMA wires. A gradient in the stiffness of the structure or the adhesive layer, on the other hand, can be added to prevent stress concentrations. It should be noted that the stress levels produced by the SMA components are very different when SMA contraction is significantly decreased and the distance to the neutral fibre is short or low SMA contraction and a long distance to the neutral fibre. The SMA parts will function at a considerably greater stress level since they are located close to the neutral axis as shown in Fig. 2(e).

2.3. 3D printing procedure

3D printing is used to fabricate structures to show the capabilities of the developed actuator. Fused deposition modelling (FDM) is the most suited technique among the 3D printing technologies used due to the high accessibility, low cost, and creation of complicated geometries with different material resources [54]. The technology prints samples layer by layer from the bottom with an abundance of material choices, from plastic to metal alloys. A filament wire is melted and quickly placed on a flat platform to create a cross-sectional feature of the desired product. The procedure is continued indefinitely, with layers on top of layers forming a solid item. The FDM prints a gripper which replicates human fingers as shown in Fig. 3(a) followed by a base structure (Fig. 3(b)) to evaluate the actuator performance. The material to print structures is black polylactic acid (PLA) filament with a 2.85 mm diameter from Ultimaker. PLA is used due to its sustainability and biodegradability. It has quite low strength and low fatigue resistance which makes it a good option for robotic applications. The Cura 4.13 software is used to slice and generate G-codes which can be read by the 3D printer. The Ultimaker S3 machine prints base structures accordingly. The structures are printed with constant parameters of 0.15 mm layer thickness, 100 % infill density, linear pattern, 210 °C nozzle temperature, 60 °C bed temperature, and 0.4 mm nozzle diameter. After printing, the actuators are mounted on the structures with screws and hexagonal nuts to evaluate their performance.

2.4. Controlling the actuator

To actuate the composite actuator, an electrical board is being built. The system is programmed using an open-source Arduino board. An electrical relay switch is used to turn on and off the actuators. In the meantime, the relay switches off the input current as soon as the actuator reaches its maximum bending. Fig. 4(a) depicts a schematic of the system. A video camera is used to capture the actuator's action, and a bending resistive sensor is used to measure the bending angles. During the procedure, the actuator is horizontally clamped, and data is captured

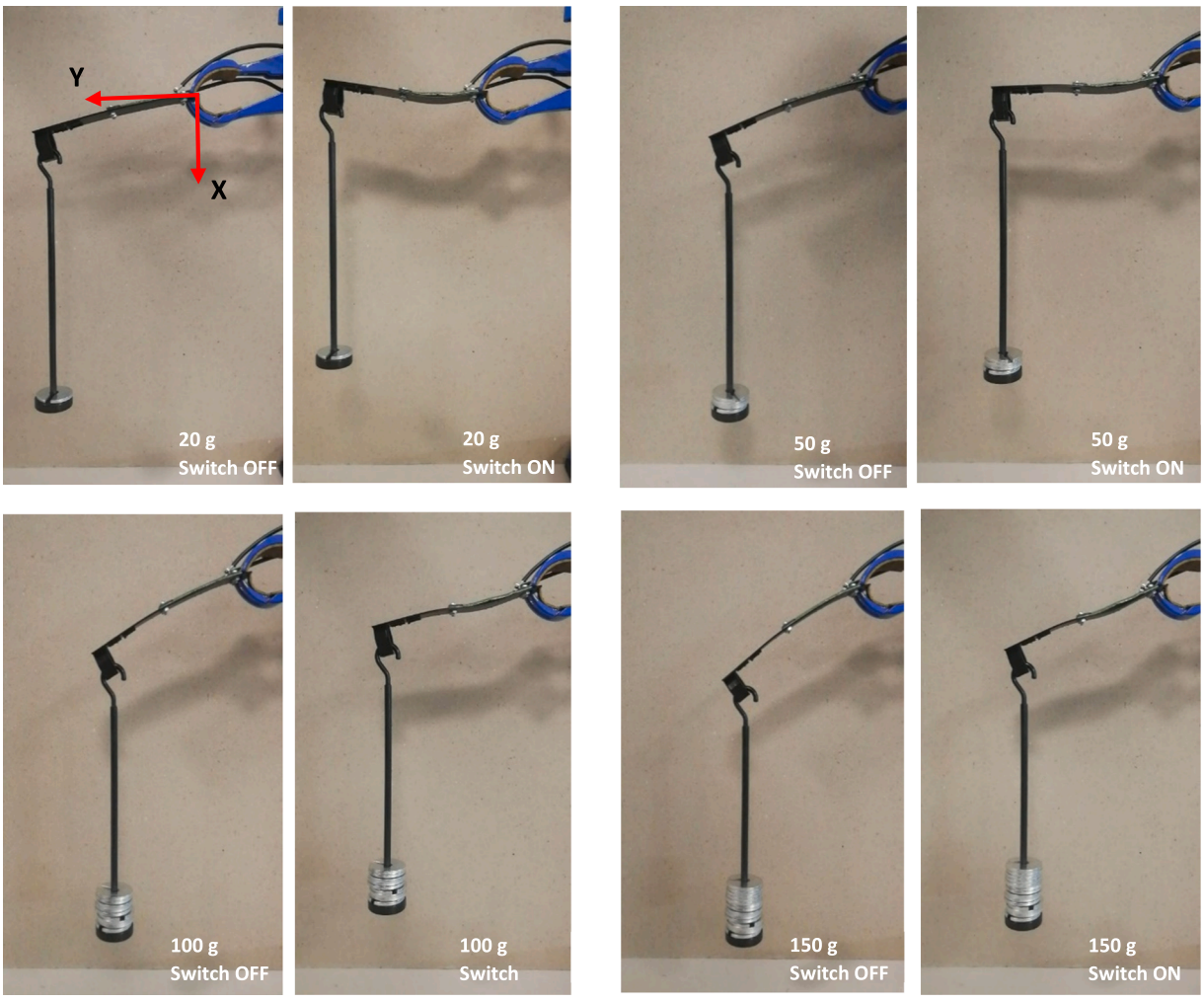

(a)

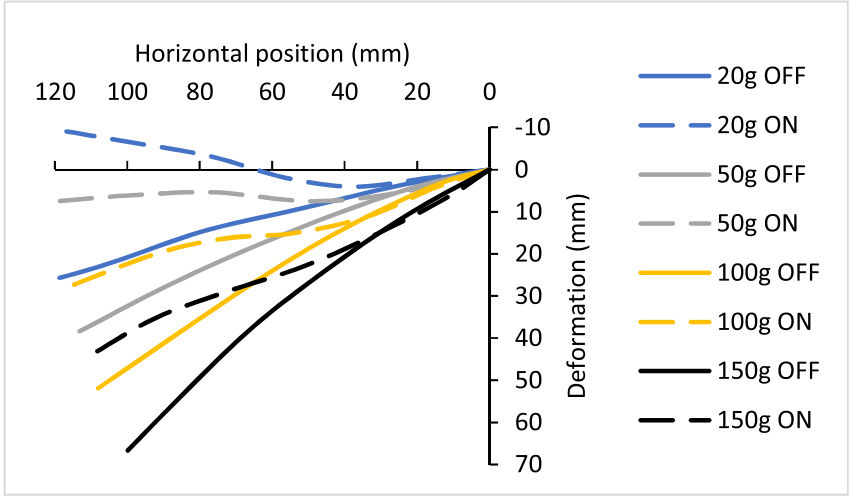

(b)

Fig. 10. (a) Lifting weights using the SMA actuator. (b) Trajectory path of the actuator module bending.

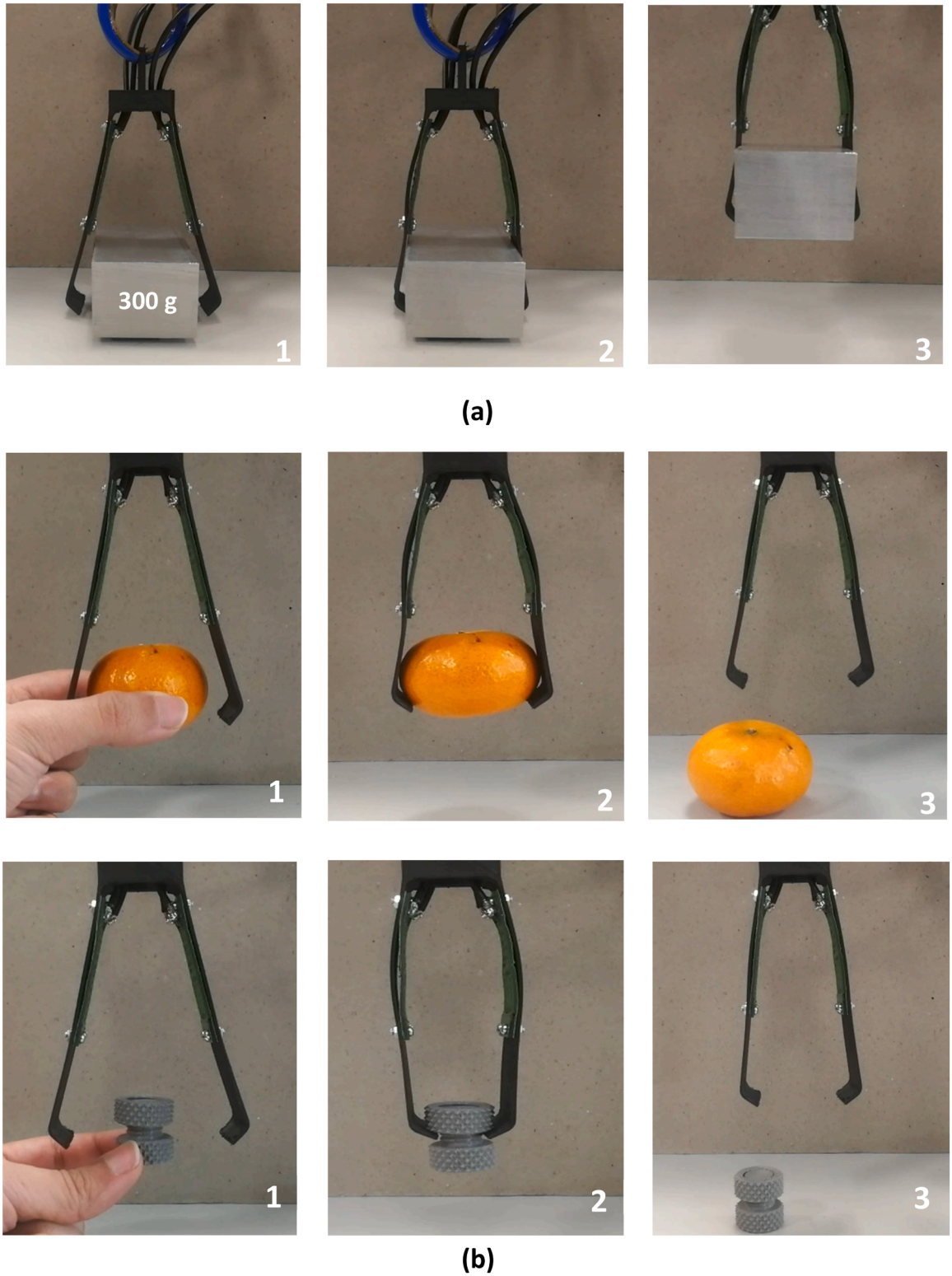

Fig. 11. Gripper in the vertical position gripping (a) rectangular metallic bulk and (b) different objects.

concurrently. The actuator's produced force is also measured using a force-sensing resistor (FSR). To acquire precise results in terms of actuator force, the force sensor is calibrated using the voltage divider approach. Fig. 4(b) shows how various weights are used to determine the force sensor's resistance. The sensor's resistance steadily decreases when the weight is increased. This calibration is used to accurately measure each actuator's tip force. Kinova software is also utilised to record motion and produce soft actuator trajectory paths.

3. Results and discussions

3.1. Training of SMA wires

Because the hybrid composite structure (epoxy resin) is cured at

room temperature, only the training process is of importance. The hot-pressing technique may actuate the SMA wires during the curing of epoxy resin. This activates the SMA wires and as a result bonding is failed. The stress-strain behaviour of NiTi SMA wire is shown in Fig. 5 (a), along with the critical stresses that initiate and complete martensite reorientation. Stress levels of more than 300 MPa have been proven to generate full martensite reorientation in this case. Also, Fig. 5(b) illustrates the contraction of a trained 50 mm SMA wire. The introduced strain might range from 1 % to 6 % depending on the application's needs. The trained SMA wire's electrical activation under continuous tensile tension is studied. A tensile test imposes a maximum strain of 12 %. The actuation capability of the SMA wire is limited by the top strain limit of the detwinning plateau of the martensitic phase, which is around 6 %. Fig. 5(b) shows that increasing the electrical current up to 3 A, increases the SMA strain up to 3.2 %. The electrical current hysteresis decreases in tandem with the increase in memory effect. The trained SMA wire is activated around 0.5 A and terminates at 3 A.

Fig. 5(c) depicts the total contraction of the material during the heating process, which reaches 3 % at 220 MPa. The hot and cold state lines are shown accordingly. The entire process is shown for both load situations, beginning with the introduction of start strain followed by the initial heating and five further heating and cooling cycles. Step 1 is the strain of the SMA wire up to 250 MPa using a load which is close to the training stress. Subsequently, step 2 is the initial heating of SMA wire around 80 °C. Step 3 is the contraction of the first heating. Steps 4 and 5 are the heating and cooling cycle up to 1.3 % strain. The second contraction noticeably increases as the stress level rises over the stress plateau in the martensitic phase. The results of the resistance test and wire temperature are shown in Fig. 5(d). The martensite start (M_s), austenite start (A_s), and austenite finish (A_f), temperatures are shown in Fig. 5(d). These critical temperatures correlate to the beginning and end of the austenite to martensite transformation during cooling, as well as the beginning and end of the martensite to austenite transformation during heating. Due to the wire's reduced contraction, the austenite phase's resistance rises. Hence, to cover a wide range of actuation fields using the resistance model, alloy system, heat treatment, and type of training must be modified in the model based on the mechanical characteristics.

The data provides information that the rising mechanical stress has essentially little effect on the austenite initiation temperature. These findings need to be taken into account the actual loading circumstances when characterising the SMA, especially as the austenite start temperature is impacted by the applied load during static loading. A contraction of 3.2 % is resulting in a deflection for an actuator with a length of 50 mm, which can withstand substantial buckling under pressure load. However, the final deformation can be greater when the number of wires in the structure is increased. The entire amount of actuation strain for wires is determined throughout this procedure.

3.2. Actuator's bending and force

In fact, it is difficult to achieve completely uniform heating and prevent elongation and contraction effects at the same time in the SMA-FRP structure. A combination of SMA with a thin structure with medium stiffness leads to a good deflection with reliable stability. The point is to place the SMA wire near the neutral axis which leads to a higher stress level in the SMA wires. Due to the highest fracture strain and the lowest modulus, epoxy resin is a great option as a base structure. Since the working temperature of the FRP structure is 150 °C, the deflection of the SMA-FRP actuator is investigated to find out the behaviour of the actuator. The bending angle of the actuator is the actuator performance that is most immediately influenced by utilizing the SMA wire. The bending actuator works because the SMA wire is arranged at the shifted location of the neutral axis when they are activated.

The deflection of the actuator with the electrical current of 3 A in different stages is shown in Fig. 6(a). The deflection of the actuator is recorded from the beginning to the end of the procedure. The maximum deflection occurs in 7 s by switching on the electrical power. After that, the electrical power is turned off and the actuator returns to its original shape. The recovery timing of the actuator is 40 s after turning the power off. Retaining to the original shape happens when the SMA wires are started to cool down with the generated force from FRP base structure. The maximum deflection of the actuator is 30 mm as recorded and shown in Fig. 6(b). Also, the bending angle is around 58°, which is good enough to be used as a gripper. The actuator creates a bending deformation with no torsion. Due to the actuator's capacity to bend freely within the restricted structure, the results reveal that the SMA's contraction is dispersed evenly on the FRP structure.

As stated in the datasheet of SMA wires, it is possible to increase the electrical current up to 6 A and more. This helps to decrease the heating time of SMA wires and results in faster bending of the actuator. No differences in bending are observed with a current of 6 A, and the actuator deflection is the same as in 3 A. However, increasing the current (I) leads to a faster heating time, which can damage the FRP. In fact, higher temperatures melt the FRP structure. The temperature is recorded to evaluate the relation between electrical current and temperature in terms of timing. The temperature of SMA alloys is around 100 °C at maximum deflection with the value of 30 mm. The response of the actuator is fast enough, however, after switching off the electrical current, it takes time for the actuator to recover to its original shape. Hence, an air compressor is used to make the actuator cool down faster after switching off the electrical source. The airflow with the pressure of 1 bar is used as soon as the electrical power is cut off. Fig. 6(c) depicts the temperature and deflection of the actuator composite in response to the electrical current of 3 A and 6 A with and without airflow. The same bending angle is also recorded for 6 A, while the bending time is reduced significantly.

The bending angle is limited because the actuator folds against a 2.5 mm thick FRP matrix. Using this method, it is feasible to select the required matrix shape in order to achieve the necessary deformation. When the FRP matrix limits the active length of the SMA wire, thicker matrixes create smaller bending deformations, reducing the utility of the actuator despite being capable of higher forces. Hence, using longer SMA wire may increase the bending angle. By utilising a longer actuator, it is also feasible to maintain the same bending deformation with a thicker matrix, allowing the actuator's force to be scaled up even further.

The results reveal that the air is highly effective in recovery form. The air decreases the recovery time of SMA-FRP from 47 s to 20 s with a 3 A electrical current. Also, the same tests are conducted for 6 A current. The experimental deformation for the actuator operating at 100 °C is 30 mm. It is also feasible to enhance the deflection by heating the SMA material to over 100 °C. The bending angle and generated force of the actuator are also recorded until the maximum bending angle is achieved. Force measurement is conducted using FSR as shown in Fig. 7(a). Fig. 7 (b) and 7(c) show the actuator can bend up 58° to and generate force up to 83 g with a 5 % error using a 3 A current.

3.3. Mechanical properties and fatigue test

The actuator's behaviour is recorded under the tensile test. Fig. 8(a) shows the force-displacement curve and behaviour of the actuator accordingly. Results indicate that the actuator is strong enough due to the existence of SMA wires to carry heavy loads without failures. The conducted results show that the failure occurs in the epoxy structure and the structure is started to tear apart after 300 N force. However, the SMA wires are not broken, and they tolerate the tensile load afterwards. Also, a fatigue test is conducted on a single actuator 500 times to determine its cyclic behaviour. A relay switch is used to turn off and turn on the current. The temperature is recorded using a thermometer and deflection is recorded using the bending sensor. The tip deflection is seen in Fig. 8(b) as it progresses 500 times. The deflection ranges between 18

and 25 mm. For the last cycles, there was no evidence of a reduction in deflection. The cooling of the system is the limiting element for the dynamic behaviour due to the temperature-based effects of SMA. The temperature is also recorded using a thermometer to evaluate the changes after 500 times (see Fig. 8(c)). The results indicate the temperature has not changed and it has been constant. This demonstrates that the system can operate for many cycles without performance degradation. For the current design, however, a further rise in SMA element contraction for temperatures beyond 100 °C might result in permanent bending of the FRP composite or damage to the actuator. The heat results in melting of the epoxy and GFRP structures as shown in Fig. 9. However, the system is able to actuate, but due to the non-uniform distribution of stress in the structure, the bending deflection is not uniform.

3.4. Actuator's performance

The actuator is mounted on the 3D-printed structure to evaluate the strength of the SMA actuator in lifting different weights. The actuator is attached to the 3D-printed sample using screws and nuts. Different weights, ranging from 20 g to 150 g, are used to be lifted up with the SMA actuator. The electrical current is set to 3 A giving enough time to lift the weights. Fig. 10 illustrates the mechanism of the actuator in lifting different weights in two conditions. The actuator can lift 150 g without any issues. However, increasing the weight loads leads to lower bending due to the restricted force. The deflection is also recorded to measure the bending of the actuator. Fig. 10(b) shows the bending trajectory path of the SMA actuator in lifting different weights. The deformation is almost 30 mm with the presence of 20 g and 50 g weights. Meanwhile, the deformation is decreased to the value of 23 mm and 22 mm when 100 g and 150 g loads are applied. Due to the high energy density of the SMA materials, which makes them less susceptible to fluctuations in loading, the changes in deformation are minor. Meanwhile, the buckling between the 3D-printed structure and the SMA actuator is visible due to the force that is generated from the actuator. This can be prevented by using glue or by applying more restrictions between SMA actuator module and 3D-printed structures. The generated force is reliable enough to be used as a soft robotic gripper.

Because of the bending deformations and tip forces described previously, a robotic gripper with the actuator is able to have better-grabbing performance. The use of an actuator and a 3D-printed gripper necessitates a routing solution in order to create a compact gripper that may be used in a variety of applications. The two parts are assembled in a modular fashion to create a gripper with the required form and number of two fingers. The advantage of this actuator is that it can be mounted on a customised structure with different shapes. The fundamental configuration investigated in this study is a two-finger grasper in parallel. The module is tested for 50 cycles with 10 s of heating and 15 s of cooling time. Due to heat accumulation inside the matrix, the bending angle increases during cooling. However, after complete cooling, the actuator restores its original unactuated bending. The actuator's grasping ability is evaluated by grabbing items of various shapes and weights with a fixed current of 3 A applied to the SMAs.

The basic purpose of soft grippers is to be able to capture items of various forms, sizes, and weights. The gripper is tested in the vertical position. The gripper can be subsequently attached to a robotic arm as the end-effector. The gripper is suited to grasp different cylindrical and rectangular items. The gripper successfully handled and released a rectangular metallic shape weighing 300 g as shown in Fig. 11(a). The objects are examined with weights ranging from 20 to 300 g (see Fig. 11 (b)). Despite the use of the SMA-FRP actuator, the developed actuator can be simply integrated into a robotic arm. The SMA wires are attached to the polymeric matrix and are in contact with the matrix throughout the SMA wire-based soft actuators. Various designs have been proposed to overcome the constraint and generate reliable deformations, but often the generated force is not enough to lift weights. Mounting this actuator into customized structures can be used in different applications.

In brief, the deflection of 30 mm appears to be confirmed by the maximum deformation of the actuator, with the possibility of additional bending. Additional bending can be achieved by modifying the 3D printed design. This result happens only if the 3D-printed structure can bear complete deflection without failure. Hence, more adhesive bonding improvements are required to have a more flexible structure. This study demonstrates the key impacts of soft actuators on the experimental description of SMA–FRP structures. The SMA wires are bonded to the framework in a repeatable manner thanks to our manufacturing technique. To alter the distance between the SMA actuator module and the 3D-printed structure, the thickness of layers beneath the actuator wires might be utilised. The bonding of the actuator to the structure needs to be investigated in the future since measurements of the actuation behaviour of various pre-strain values reveal the SMA wire's considerably increased actuator performance.

4. Conclusion

Because of the high actuation stress of SMA, they are suitable candidates for combination with high-performance FRP composites. In this study, a soft SMA-FRP actuator was developed, which can be mounted on various structures. Pre-straining of SMA wires was discussed to programme the wires before inserting them into the FRP matrix. Assembly is simpler since only two electrical connections are required. An electrical current with a value of 3 A was used to actuate the actuator. The performance of bending and deformation of the actuator was evaluated. Tensile tests were conducted on SMA wires and SMA-FRP structure to investigate their properties. An electrical board was developed to control the actuator and record the bending angle and generated force. A bending angle of 58° and 86 g force were achieved with 30 mm maximum deformation. The recovery time was also investigated, and airflow cooling was highly effective in reducing cooling time. The fatigue test of the actuator in terms of deflection and temperature is also evaluated using 500 cycles. The FDM process was used to print a gripper inspired by human fingers and a structure for lifting weights. The actuator was able to lift the weights from 20 g up to 300 g with different shapes. Also, the SMA actuator was mounted on the 3D-printed gripper and was able to pick and release the objects without issues. The proposed actuator can be used in different applications due to the promising features such as high bending and the capability of mounting on different structures. Further development of this actuator in terms of a softer actuator with reasonable bending and stiffness can be investigated as well. The focus of future development will be on identifying and implementing the most promising applications that will considerably boost the product's value.

CRediT authorship contribution statement

Mohammadreza Lalegani Dezaki: Conceptualization, Investigation, Methodology, Data curation, Formal analysis, Experiment, Writing – original draft. **Mahdi Bodaghi:** Methodology, Project administration, Supervision, Writing – review & editing. **Ahmad Serjoue:** Critical evaluation, Writing – review & editing. **Shukri Afazov:** Critical evaluation, Writing – review & editing. **Ali Zolfagharian:** Critical evaluation, Writing – review & editing.

Declaration of Competing Interest

The authors declare that they have no known competing financial interests or personal relationships that could have appeared to influence the work reported in this paper.

References

[1] B. Grossi, H. Palza, J.C. Zagal, C. Falcón, G. During, Metarpillar: Soft robotic locomotion based on buckling-driven elastomeric metamaterials, Mater. Des. 212 (2021), 110285, https://doi.org/10.1016/j.matdes.2021.110285.

[2] S. Coyle, C. Majidi, P. LeDuc, K.J. Hsia, Bio-inspired soft robotics: material selection, actuation, and design, Extrem. Mech. Lett. 22 (2018) 51–59, https://doi.org/10.1016/j.eml.2018.05.003.

[3] E. Yarali, M. Baniasadi, A. Zolfagharian, M. Chavoshi, F. Arefi, M. Hossain, A. Bastola, M. Ansari, A. Foyouzat, A. Dabbagh, M. Ebrahimi, M.J. Mirzaali, M. Bodaghi, Magneto-/ electro-responsive polymers toward manufacturing, characterization, and biomedical/ soft robotic applications, Appl. Mater. Today 26 (2022), 101306, https://doi.org/10.1016/j.apmt.2021.101306.

[4] F. Schmitt, O. Piccin, L. Barbé, B. Bayle, Soft robots manufacturing: a review, Front. Robot. AI 5 (2018), https://doi.org/10.3389/frobt.2018.00084.

[5] N. El-Atab, R.B. Mishra, F. Al-Modaf, L. Joharji, A.A. Alsharif, H. Alamoudi, M. Diaz, N. Qaiser, M.M. Hussain, Soft actuators for soft robotic applications: a review, Adv. Intell. Syst. 2 (2020), 2000128, https://doi.org/10.1002/aisy.202000128.

[6] J. Shintake, V. Cacucciolo, D. Floreano, H. Shea, Soft robotic grippers, Adv. Mater. 30 (2018), 1707035, https://doi.org/10.1002/adma.201707035.

[7] W. Wang, Y. Tang, C. Li, Controlling bending deformation of a shape memory alloy-based soft planar gripper to grip deformable objects, Int. J. Mech. Sci. 193 (2021), 106181, https://doi.org/10.1016/j.ijmecsci.2020.106181.

[8] F. Spina, A. Pouryazdan, J.C. Costa, L.P. Cuspinera, N. Münzenrieder, Directly 3D-printed monolithic soft robotic gripper with liquid metal microchannels for tactile sensing, Flex. Print. Electron. 4 (2019), 035001, https://doi.org/10.1088/2058-8585/ab3384.

[9] A. Zolfagharian, A.Z. Kouzani, S.Y. Khoo, B. Nasri-Nasrabadi, A. Kaynak, Development and analysis of a 3D printed hydrogel soft actuator, Sens. Actuators A: Phys. 265 (2017) 94–101, https://doi.org/10.1016/j.sna.2017.08.038.

[10] L. Jing, K. Li, H. Yang, P.-Y. Chen, Recent advances in integration of 2D materials with soft matter for multifunctional robotic materials, Mater. Horiz. 7 (2020) 54–70, https://doi.org/10.1039/C9MH01139K.

[11] P. Boyraz, G. Runge, A. Raatz, An overview of novel actuators for soft robotics, Actuators 7 (2018) 48, https://doi.org/10.3390/act7030048.

[12] S. Zaidi, M. Maselli, C. Laschi, M. Cianchetti, Actuation technologies for soft robot grippers and manipulators: a review, Curr. Robot. Rep. 2 (2021) 355–369, https://doi.org/10.1007/s43154-021-00054-5.

[13] M. Bodaghi, A.R. Damanpack, M.M. Aghdam, M. Shakeri, Active shape/stress control of shape memory alloy laminated beams, Compos. Part B: Eng. 56 (2014) 889–899, https://doi.org/10.1016/j.compositesb.2013.09.018.

[14] J. Li, W. Chang, Q. Li, Soft robot with a novel variable friction design actuated by SMA and electromagnet, Smart Mater. Struct. 27 (2018), 115020, https://doi.org/10.1088/1361-665X/aae412.

[15] W. Wang, H. Rodrigue, H.-I. Kim, M.-W. Han, S.-H. Ahn, Soft composite hinge actuator and application to compliant robotic gripper, Compos. Part B: Eng. 98 (2016) 397–405, https://doi.org/10.1016/j.compositesb.2016.05.030.

[16] S. Kim, C. Laschi, B. Trimmer, Soft robotics: a bioinspired evolution in robotics, Trends Biotechnol. 31 (2013) 287–294, https://doi.org/10.1016/j.tibtech.2013.03.002.

[17] S.G. Fitzgerald, G.W. Delaney, D. Howard, A review of jamming actuation in soft robotics, Actuators 9 (2020) 104, https://doi.org/10.3390/act9040104.

[18] L. Marechal, P. Balland, L. Lindenroth, F. Petrou, C. Kontovounisios, F. Bello, Toward a common framework and database of materials for soft robotics, Soft Robot. 8 (2021) 284–297, https://doi.org/10.1089/soro.2019.0115.

[19] W.-S. Chu, K.-T. Lee, S.-H. Song, M.-W. Han, J.-Y. Lee, H.-S. Kim, M.-S. Kim, Y.-J. Park, K.-J. Cho, S.-H. Ahn, Review of biomimetic underwater robots using smart actuators, Int. J. Precis. Eng. Manuf. 13 (2012) 1281–1292, https://doi.org/10.1007/s12541-012-0171-7.

[20] A. Nespoli, S. Besseghini, S. Pittaccio, E. Villa, S. Viscuso, The high potential of shape memory alloys in developing miniature mechanical devices: a review on shape memory alloy mini-actuators, Sens. Actuators A: Phys. 158 (2010) 149–160, https://doi.org/10.1016/j.sna.2009.12.020.

[21] M.C. Yuen, R.A. Bilodeau, R.K. Kramer, Active variable stiffness fibers for multifunctional robotic fabrics, IEEE Robot. Autom. Lett. 1 (2016) 708–715, https://doi.org/10.1109/LRA.2016.2519609.

[22] V. Birman, Review of mechanics of shape memory alloy structures, Appl. Mech. Rev. 50 (1997) 629–645, https://doi.org/10.1115/1.3101674.

[23] C. Simoneau, P. Terriault, S. Lacasse, V. Brailovski, Adaptive composite panel with embedded SMA actuators: modeling and validation, Mech. Based Des. Struct. Mach. 42 (2014), https://doi.org/10.1080/15397734.2013.864246.

[24] L. Mizzi, A. Spaggiari, E. Dragoni, Design-oriented modelling of composite actuators with embedded shape memory alloy, Compos. Struct. 213 (2019), https://doi.org/10.1016/j.compstruct.2019.01.057.

[25] P. Ghosh, A. Rao, A.R. Srinivasa, Design of multi-state and smart-bias components using shape memory alloy and shape memory polymer composites, Mater. Des. 44 (2013) 164–171, https://doi.org/10.1016/j.matdes.2012.05.063.

[26] K. Choi, S.J. Park, M. Won, C.H. Park, Soft fabric muscle based on thin diameter SMA springs, Smart Mater. Struct. 31 (2022), 055020, https://doi.org/10.1088/1361-665X/ac6550.

[27] L. Mizzi, A. Spaggiari, E. Dragoni, Design of shape memory alloy sandwich actuators: an analytical and numerical modelling approach, Smart Mater. Struct. 29 (2020), 085027, https://doi.org/10.1088/1361-665X/ab972e.

[28] P. Bettini, M. Riva, G. Sala, L. di Landro, A. Airoldi, J. Cucco, Carbon fiber reinforced smart laminates with embedded SMA actuators-part I: embedding techniques and interface analysis, J. Mater. Eng. Perform. 18 (2009), https://doi.org/10.1007/s11665-009-9384-z.

[29] J. Mohd Jani, M. Leary, A. Subic, M.A. Gibson, A review of shape memory alloy research, applications and opportunities, Mater. Des. (1980-2015) 56 (2014) 1078–1113, https://doi.org/10.1016/j.matdes.2013.11.084.

[30] U. Icardi, Large bending actuator made with SMA contractile wires: theory, numerical simulation and experiments, Compos. Part B Eng. 32 (2001) 259–267, https://doi.org/10.1016/S1359-8368(00)00062-7.

[31] Y. Du, B. Liu, M. Xu, E. Dong, S. Zhang, J. Yang, Dynamic characteristics of planar bending actuator embedded with shape memory alloy, Mechatronics 25 (2015) 18–26, https://doi.org/10.1016/j.mechatronics.2014.11.001.

[32] H. Rodrigue, W. Wang, B. Bhandari, M.-W. Han, S.-H. Ahn, SMA-based smart soft composite structure capable of multiple modes of actuation, Compos. Part B: Eng. 82 (2015) 152–158, https://doi.org/10.1016/j.compositesb.2015.08.020.

[33] Y. Haibin, K. Cheng, L. Junfeng, Y. Guilin, Modeling of grasping force for a soft robotic gripper with variable stiffness, Mech. Mach. Theory 128 (2018) 254–274, https://doi.org/10.1016/j.mechmachtheory.2018.05.005.

[34] J.-H. Lee, Y.S. Chung, H. Rodrigue, Long shape memory alloy tendon-based soft robotic actuators and implementation as a soft gripper, Sci. Rep. 9 (2019) 11251, https://doi.org/10.1038/s41598-019-47794-1.

[35] M. Modabberifar, M. Spenko, A shape memory alloy-actuated gecko-inspired robotic gripper, Sens. Actuators A Phys. 276 (2018) 76–82, https://doi.org/10.1016/j.sna.2018.04.018.

[36] M. Liu, L. Hao, W. Zhang, Z. Zhao, A novel design of shape-memory alloy-based soft robotic gripper with variable stiffness, Int. J. Adv. Robot. Syst. 17 (2020), 172988142090781, https://doi.org/10.1177/1729881420907813.

[37] D. Niu, D. Li, J. Chen, M. Zhang, B. Lei, W. Jiang, J. Chen, H. Liu, SMA-based soft actuators with electrically responsive and photoresponsive deformations applied in soft robots, Sens. Actuators A: Phys. 341 (2022), 113516, https://doi.org/10.1016/j.sna.2022.113516.

[38] P. Alam, D. Mamalis, C. Robert, C. Floreani, C.M.Ó. Brádaigh, The fatigue of carbon fibre reinforced plastics - a review, Compos. Part B Eng. 166 (2019) 555–579, https://doi.org/10.1016/j.compositesb.2019.02.016.

[39] Y. Yang, Y. Wang, T. Yao, X. Feng, A flexible carbon fibre-based electrothermal film for fast actuation of shape memory alloy sheets, Smart Mater. Struct. 31 (2022), 045019, https://doi.org/10.1088/1361-665X/ac5808.

[40] P.K. Kumar, C. Caer, G. Atkinson, E. Patoor, D.C. Lagoudas, The influence of stress and temperature on the residual strain generated during pseudoelastic cycling of NiTi SMA wires, in: Z. Ounaies, S.S. Seelecke (Eds.), Behav. Mech. Multifunct. Mater. Compos. (2011) 79781, https://doi.org/10.1117/12.881994.

[41] A. Riccio, A. Sellitto, S. Ameduri, A. Concilio, M. Arena, Shape memory alloys (SMA) for automotive applications and challenges, in: Shape Memory Alloy Engineering, Elsevier, 2021, pp. 785–808, https://doi.org/10.1016/B978-0-12-819264-1.00024-8.

[42] C.A. Rogers, C. Liang, C.R. Fuller, Modeling of shape memory alloy hybrid composites for structural acoustic control, J. Acoust. Soc. Am. 89 (1991) 210–220, https://doi.org/10.1121/1.400503.

[43] C.A. Rogers, Active vibration and structural acoustic control of shape memory alloy hybrid composites: experimental results, J. Acoust. Soc. Am. 88 (1990) 2803–2811, https://doi.org/10.1121/1.399683.

[44] K. Mehar, P.K. Mishra, S.K. Panda, Numerical investigation of thermal frequency responses of graded hybrid smart nanocomposite (CNT-SMA-Epoxy) structure, Mech. Adv. Mater. Struct. 28 (2021) 2242–2254, https://doi.org/10.1080/15376494.2020.1725193.

[45] H. Lei, Z. Wang, B. Zhou, L. Tong, X. Wang, Simulation and analysis of shape memory alloy fiber reinforced composite based on cohesive zone model, Mater. Des. 40 (2012) 138–147, https://doi.org/10.1016/j.matdes.2012.03.037.

[46] A. Cohades, V. Michaud, Shape memory alloys in fibre-reinforced polymer composites, Adv. Ind. Eng. Polym. Res. 1 (2018) 66–81, https://doi.org/10.1016/j.aiepr.2018.07.001.

[47] M. Ashir, A. Nocke, C. Theiss, C. Cherif, Development of adaptive hinged fiber reinforced plastics based on shape memory alloys, Compos. Struct. 170 (2017) 243–249, https://doi.org/10.1016/j.compstruct.2017.03.031.

[48] J. Mersch, M. Bruns, A. Nocke, C. Cherif, G. Gerlach, High-displacement, fiber-reinforced shape memory alloy soft actuator with integrated sensors and its equivalent network model, Adv. Intell. Syst. 3 (2021), 2000221, https://doi.org/10.1002/aisy.202000221.

[49] C.J. de Araújo, L.F.A. Rodrigues, J.F. Coutinho Neto, R.P.B. Reis, Fabrication and static characterization of carbon-fiber-reinforced polymers with embedded NiTi shape memory wire actuators, Smart Mater. Struct. 17 (2008), 065004, https://doi.org/10.1088/0964-1726/17/6/065004.

[50] P.K. Kumar, D.C. Lagoudas, Introduction to Shape Memory Alloys, in: Shape Memory Alloys, Springer US, Boston, MA, 2008, pp. 1–51, https://doi.org/10.1007/978-0-387-47685-8_1.

[51] R. Britz, P. Motzki, Analysis and evaluation of bundled SMA actuator wires, Sens. Actuators A Phys. 333 (2022), 113233, https://doi.org/10.1016/j.sna.2021.113233.

[52] H. Asadi, M. Bodaghi, M. Shakeri, M.M. Aghdam, Nonlinear dynamics of SMA-fiber-reinforced composite beams subjected to a primary/secondary-resonance

excitation, Acta Mech. 226 (2015) 437–455, https://doi.org/10.1007/s00707-014-1191-4.
[53] V. Choyal, S. Khan, P.S.S. Mani, I.A. Palani, P. Singh, Active and passive multicycle actuation characteristics of shape memory alloy-based adaptive composite structures, Smart Mater. Struct. 30 (2021), 095022, https://doi.org/10.1088/1361-665X/ac177d.
[54] M. Lalegani Dezaki, M.K.A. Mohd Ariffin, S. Hatami, An overview of fused deposition modelling (FDM): research, development and process optimisation, Rapid Prototyp. J. 27 (2021) 562–582, https://doi.org/10.1108/RPJ-08-2019-0230.

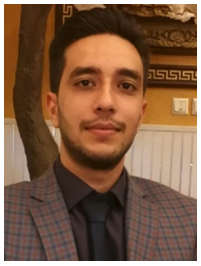

Mohammadreza Lalegani Dezaki received his MSc degree in Manufacturing Systems Engineering from Universiti Putra Malaysia (UPM). He has published several papers in the field of 3D printing. In 2021, He was awarded a Ph.D. Studentship issued by Nottingham Trent University (NTU). His current research interests involve 3D printing and smart soft actuators for soft robots.

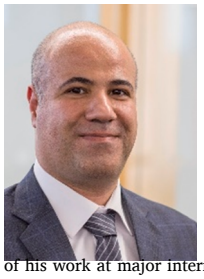

Dr Mahdi Bodaghi (BSc, MSc, Ph.D., PGCAP, FHEA, CEng, MIMechE) is a Senior Lecturer in the Department of Engineering at Nottingham Trent University. He is also the founder and director of the 4D Materials & Printing Lab that hosts a broad portfolio of projects focusing on the electro-thermo-mechanical multi-scale behaviours of smart materials, soft robots, and 3D/4D printing technologies. His vast experience and research on smart materials and additive manufacturing has led him to co-found the 4D Printing Society and to co-edit the book series- Smart Materials in Additive Manufacturing. His research has also resulted in the publication of over 140 scientific papers in prestigious journals as well as the presentation of his work at major international conferences. Mahdi has also served as Chairman and member of Scientific Committees for 10 International Conferences, as Guest Editor for 10 Journals, as Editorial Board Member for 10 scientific Journals, and as Reviewer for over 140 Journals. Mahdi's research awards include the Best Doctoral Thesis Award of 2015, 2016 CUHK Postdoctoral Fellowship, the Annual Best Paper Award in Mechanics and Material Systems presented by the American Society of Mechanical Engineers in 2017, 2018 Horizon Postdoctoral Fellowship Award, and 2021 IJPEM-GT Contribution Award recognized by the Korea Society for Precision Engineering.

Dr Ahmad Serjouei completed his BSc (Mech. Eng.) at Isfahan University of Technology (IUT), Iran in 2007. He obtained his MEng and PhD from Nanyang Technological University (NTU), Singapore in 2009 and 2014. He is a Chartered Engineer (CEng) and holds Fellow of Higher Education Academy (FHEA) and Postgraduate Certificate in Academic Practice (PGCAP) certificates for teaching. He has been a senior lecturer at Nottingham Trent University (NTU), UK since 2019. His research interests include mechanics of materials, 3D and 4D printing, metal additive manufacturing, smart materials and structures, and soft actuation.

Dr Shukri Afazov is a chartered mechanical engineer who holds a Ph.D. in mechanical engineering from the University of Nottingham. He delivered fundamental and applied research during his PhD and postdoctoral period of six years at the University of Nottingham (TRL1–6). Shukri joined Nottingham Trent University in 2019 to support the development of the next generation of engineers in Mechanical, Materials, Manufacturing & Digital Engineering. His research vision is to deliver innovative solutions and their adoption in industry through collaboration. His research areas are advanced manufacturing technologies, structural integrity of systems, digital manufacturing, and digital twins for design, manufacture and product lifecycle management. He is the module leader for "Materials and Manufacturing" and "Foundation Engineering".

Dr Ali Zolfagharian (BSc, MSc, Ph.D., ADPRF, GCHE) is a Senior Lecturer in the Faculty of Science, Engineering and Built Environment, School of Engineering at Deakin University, Australia. He has been among the 2 % top cited scientists listed by Stanford University and Elsevier (2020), the Alfred Deakin Medallist for Best Doctoral Thesis (2019), and the Alfred Deakin Postdoctoral Fellowship Awardee (2018). He has been directing 4D Printing and Robotic Materials lab at Deakin University since 2018. Ali is co-founder of the 4D Printing Society, co-editor of the Smart Materials in Additive Manufacturing book series published by Elsevier, and a technical committee member of 5 international conferences. From 2020–2022, he has received more than AUD 200k research funds from academic and industrial firms. Ali's research outputs on flexible manipulators, soft grippers, robotic materials 3D/4D printing, and bioprinting include 74 articles, 15 special issues, being editor of 2 journals, and 5 books.